Multishell diffusion-weighted MRI characterization of chronic active lesions in Multiple Sclerosis

Anna Stölting[1], Colin Vanden Bulcke[1,2], Dominika Jelinkova[1], Gaëtan Duchêne[3], Laurence Dricot[4], Benoit Macq[2], Pietro Maggi[1]

1. Neuroinflammation Imaging Lab (NIL), Institute of NeuroScience, Université catholique de Louvain, Brussels, Belgium
2. ICTEAM Institute, Université catholique de Louvain, Louvain-la-Neuve, Belgium
3. MR applications, GE HealthCare, Diegem, Belgium
4. Institute of NeuroScience, Université catholique de Louvain, Brussels, Belgium

Introduction

Chronic active multiple sclerosis (MS) lesions, seen on susceptibility-weighted (SWI) MRI as Paramagnetic Rim Lesions (PRL), are associated with increased clinical disability and axonal damage.[1,2] Diffusion MRI (dMRI) can characterize in vivo PRL's tissue damage,[3] however the tissue microstructure specificity of dMRI models is limited. Here, we characterized PRL's microstructure using 4 different models, including one novel dMRI model: Microstructure Fingerprinting (MF).[4] Compared to other commonly used diffusion models, which are based on the optimization of complex analytical equations, MF uses Monte-Carlo simulations of water molecule diffusion in complex 3D white matter (WM) numerical configurations.

Methods

In 44 MS patients (27 relapsing-remitting, 11 secondary progressive, 6 primary progressive) 367 lesions (202 PRL and 165 non-PRL) were detected on 3T high resolution Susceptibility-Weighted Echo Planar Imaging (SWI-EPI)[5] images and segmented on FLuid Attenuated Inversion Recovery (FLAIR) images. Each subject underwent a multishell diffusion-weighted imaging (TR=4842 ms, TE=77 ms, Δ=35.7 ms, δ=22.9 ms, 64 gradients at b=1000, 32 at b=2000,3000,5000 s/mm^2). For each lesion, we calculated the volume, we computed quantitative T1 values on Magnetization Prepared 2 Rapid Acquisition Gradient Echoes (MP2RAGE) derived T1 maps,[6] and we extracted diffusion parameters using 4 dMRI models: Diffusion Tensor Imaging (DTI),[7] Neurite Orientation Dispersion and Density Imaging (NODDI),[8] DIstribution of Anisotropic MicrOstructural eNvironments in DWI (DIAMOND)[9] and MF.

Results

PRL were bigger ($p<0.001$) and featured higher T1-values ($p<0.001$) vs non-PRL. The DTI and DIAMOND models showed lower fractional anisotropy, higher mean diffusivity and radial diffusivity in PRL vs non-PRL; NODDI and MF models showed respectively lower neurite density index and lower weighted fibre volume fraction ($p<0.001$), suggesting impaired axonal integrity/density in PRL vs non-PRL (**Table 1**, **Figure 1**).

Conclusion

Consistent with previous data,[3,10] we show that PRL are characterized by higher axonal damage when compared to non-PRL. Results derived from the MF model are in line with those obtained with DTI, NODDI and DIAMOND, suggesting that this novel dMRI model can be used to study MS lesion pathology. As an advantage, the MF framework allows further methodological improvement, by computing more complex models to represent the microstructure of the brain WM.[4]

Disclosures

Authors have no relevant disclosures related to this submission.

	PRL *Mean ± SD*	**non-PRL** *Mean ± SD*	*p*
Volume, mm^3	228,673 ± 290,301	102,998 ± 112,540	< 0,001
T1, ms	1529,872 ± 284,678	1236,189 ± 217,452	< 0,001
DTI_AD, mm^2/s	0,00101 ± 0,00018	0,00096 ± 0,00019	< 0,001
DTI_FA	0,35872 ± 0,11089	0,44450 ± 0,12704	< 0,001
DTI_MD, mm^2/s	0,00074 ± 0,00014	0,00064 ± 0,00013	< 0,001
DTI_RD, mm^2/s	0,00060 ± 0,00015	0,00047 ± 0,00014	< 0,001
NODDI_fExtra	0,58044 ± 0,10657	0,48462 ± 0,10705	< 0,001
NODDI_NDI	0,27335 ± 0,08745	0,33077 ± 0,10099	< 0,001
NODDI_fIso	0,14599 + 0,10826	0,18461 ± 0,09603	< 0,001
NODDI_odi	0,25121 ± 0,08352	0,23366 ± 0,07619	0,097
DIAMOND_wAD, mm^2/s	0,00182 ± 0,00029	0,00175 ± 0,00028	0,018
DIAMOND_wFA	0,54310 ± 0,12855	0,63083 ± 0,13551	< 0,001
DIAMOND_wMD, mm^2/s	0,00107 ±0,00016	0,00095 ± 0,00017	< 0,001
DIAMOND_wRD, mm^2/s	0,00070 ± 0,00018	0,00054 ±0,00020	< 0,001
MF_frac_CSF	0,26621 ± 0,15471	0,20683 ± 0,14503	< 0,001
MF_frac_ftot	0,73357 ± 0,15500	0,79317 ± 0,14503	< 0,001
MF_fvf_tot	0,14803 ± 0,06889	0,20792 ± 0,08798	< 0,001
MF_wfvf	0,19508 ± 0,06413	0,25581 ± 0,08374	< 0,001

Table 1 *- Mean volume, T1 times and diffusion parameters of DTI, NODDI, DIAMOND and MF models for PRL and non-PRL lesions.*
Abbreviations: **DTI_AD:** DTI Axial Diffusivity **DTI_FA:** DTI Fractional Anisotropy **DTI_MD:** DTI Mean Diffusivity **DTI_RD:** DTI Radial Diffusivity **NODDI_fExtra:** NODDI Fraction Extracellular **NODDI_NDI:** NODDI Neurite Density Index **NODDI_fIso:** NODDI CSF Compartment **NODDI_odi:** NODDI Orientation Dispersion Index **DIAMOND_wAD:** DIAMOND Axial Diffusivity **DIAMOND_wFA:** DIAMOND Fractional Anisotropy **DIAMOND_wMD:** DIAMOND Mean Diffusivity **DIAMOND_wRD:** DIAMOND Radial Diffusivity **MF_frac_CSF:** MF fraction CSF **MF_frac_ftot:** MF Total Tissue Fraction **MF_fvf_tot:** MF Total Fibre Volume Fraction **MF_wfvf:** MF Weighted Fibre Volume Fraction

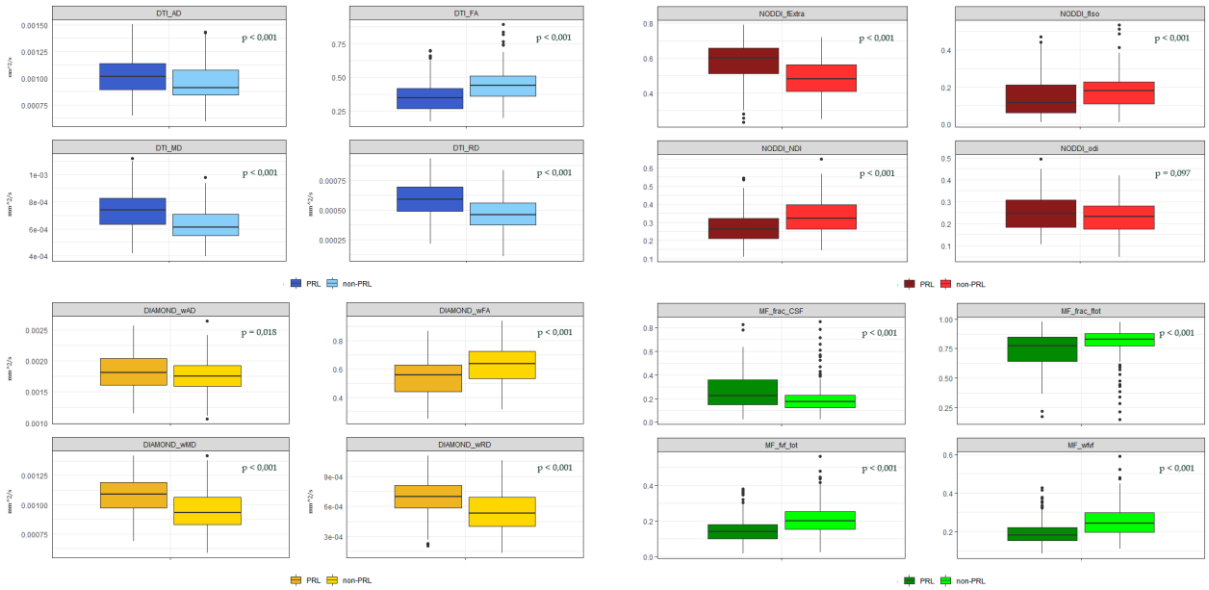

Figure 1 *– Boxplot of average DTI (blue), NODDI (red), DIAMOND (yellow) and MF (green) dMRI model parameters in PRL and non-PRL lesions.*
Abbreviations: **DTI_AD:** DTI Axial Diffusivity **DTI_FA:** DTI Fractional Anisotropy **DTI_MD:** DTI Mean Diffusivity **DTI_RD:** DTI Radial Diffusivity **NODDI_fExtra:** NODDI Fraction Extracellular **NODDI_NDI:** NODDI Neurite Density Index **NODDI_fIso:** NODDI CSF Compartment **NODDI_odi:** NODDI Orientation Dispersion Index **DIAMOND_wAD:** DIAMOND Axial Diffusivity **DIAMOND_wFA:** DIAMOND Fractional Anisotropy **DIAMOND_wMD:** DIAMOND Mean Diffusivity **DIAMOND_wRD:** DIAMOND Radial Diffusivity **MF_frac_CSF:** MF fraction CSF **MF_frac_ftot:** MF Total Tissue Fraction **MF_fvf_tot:** MF Total Fibre Volume Fraction **MF_wfvf:** MF Weighted Fibre Volume Fraction

References

1. Absinta, M. *et al.* Association of Chronic Active Multiple Sclerosis Lesions With Disability In Vivo. *JAMA Neurol.* **76**, 1474–1483 (2019).
2. Maggi, P. *et al.* Chronic White Matter Inflammation and Serum Neurofilament Levels in Multiple Sclerosis. *Neurology* **97**, e543–e553 (2021).
3. Rahmanzadeh, R. *et al.* Myelin and axon pathology in multiple sclerosis assessed by myelin water and multi-shell diffusion imaging. *Brain J. Neurol.* **144**, 1684–1696 (2021).
4. Rensonnet, G. *et al.* Towards microstructure fingerprinting: Estimation of tissue properties from a dictionary of Monte Carlo diffusion MRI simulations. *NeuroImage* **184**, 964–980 (2019).
5. Sati, P. *et al.* Rapid, high-resolution, whole-brain, susceptibility-based MRI of multiple sclerosis. *Mult. Scler. J.* **20**, 1464–1470 (2014).
6. Marques, J. P. *et al.* MP2RAGE, a self bias-field corrected sequence for improved segmentation and T1-mapping at high field. *NeuroImage* **49**, 1271–1281 (2010).
7. Basser, P. J., Mattiello, J. & Lebihan, D. Estimation of the Effective Self-Diffusion Tensor from the NMR Spin Echo. *J. Magn. Reson. B* **103**, 247–254 (1994).
8. Zhang, H., Schneider, T., Wheeler-Kingshott, C. A. & Alexander, D. C. NODDI: Practical in vivo neurite orientation dispersion and density imaging of the human brain. *NeuroImage* **61**, 1000–1016 (2012).
9. Scherrer, B. *et al.* Characterizing the distribution of anisotropic micro-structural environments with diffusion-weighted imaging (DIAMOND). *Med. Image Comput. Comput.-Assist. Interv. MICCAI Int. Conf. Med. Image Comput. Comput.-Assist. Interv.* **16**, 518–526 (2013).
10. Rahmanzadeh, R. *et al.* A New Advanced MRI Biomarker for Remyelinated Lesions in Multiple Sclerosis. *Ann. Neurol.* **92**, 486–502 (2022).